Upwelling characteristics during El Nino 2015 in Maluku Sea

A S Atmadipoera[1*], Z Khairunnisa[1], D W Kusuma[2]

[1]Department of Marine Science and Technology, Bogor Agricultural University [2]Marine Observation and Research Center (BPOL-KKP), Bali
*e-mail: atmadipoera_itk@ipb.ac.id

Abstract. Investigation of upwelling characteristics in Banggai-Maluku Sea (BMS) during super El Nino 2015 event and its interannual variation related to ENSO used validated INDESO model output and satellite imagery datasets between 2008 and 2015. The result shows the upwelling episode occurs during the Southeast Monsoon period from June to October, and its maximum in September. It is mainly forced by fully developed southerly monsoon winds, dragging surface water northward similar to the wind direction since the effect of Coriolis vanishes near the equator. Warm surface water in the center upwelling is replaced by upwelled colder water from about 60 m, which evolves from southern to northern region then curving to northeastern due to the boundary of Sulawesi mainland. Upwelling characteristics in 2015 event is indicated by drastic changes in ocean-atmosphere variables, such as increased northward meridional winds/ infrared heat flux/ transport volume, decreased sensible heat flux/ mixed layer depth, upwelled 26°C isotherm from 60 m depth to surface, and blooming surface chlorophyll-a. Between 2008 and 2015, upwelling intensity in 2015 was the most powerful (index: -5.35), in contrast to upwelling intensity during 2010 strong La Nina event (+0.27). Hence, ENSO influences significantly on fluctuation of upwelling intensity in BMS.

1. Introduction

Upwelling is an oceanographic phenomenon of which deeper and colder water mass rises towards the surface, replacing warmer surface water mass [1]. There are three types of upwelling: coastal, equatorial, and polar upwelling. Coastal upwelling happens when water depletion occurs in upper layer and space is vacated by offshore drift, which is affected by wind and Ekman drift [2]. The trade winds generate equatorial upwelling, which leads to water mass uplifting to both northern and southern hemispheres, while polar upwelling happens near ice edge. There are several factors affected upwelling, such as wind, topographic condition, length and curvature of the coast [20].

Rising water mass in upwelling affects water mass characteristics. Upwelled water mass has cooler temperature with higher salinity, thus affecting surface temperature and salinity distribution in the region. It is also rich of nutrients, related to higher primary productivity [19]. Therefore, upwelling drives important biological consequences, and from there related to marine fisheries [12]. It also alters weather as [19] stated that weather onshore of upwelling region tend to be foggy with low stratus clouds, along with stable stratified atmosphere, less convection, and less rain.

Several methods are be able to understand ocean phenomenon such as upwelling. In-situ hydrographic measurement can be carried out to provide information on oceanographic conditions, such as temperature-salinity, nutrients, and chlorophyll-a distribution, conducted by [20] and [21] in Makassar upwelling region, based on MAJAFLOX Cruise 2015. Recently, remote sensing and numerical model has been widely used to complement field measurement, due to its inexpensive cost and larger spatial data retrieval, which depicts actual condition. Using remote sensing data, [3] and [4], studied upwelling in southern Makassar Strait and Gulf of Tomini, respectively. Both studies show SST cooling and chlorophyll-a blooming occurred during Southeast Monsoon, associated with the southerly

winds fields. Numerical ocean model is also used to study upwelling, such as research on southern Makassar Strait by [5] using numerical model to analyze main upwelling generating force, and [6] using carbon-based productivity model to identify upwelling effect to primary productivity in Indonesian Sea. Recent hydrographic observation in southern Makassar reported upwelled water layer was found from subsurface (60 m) layer to surface as indicated by surfacing 25°C isotherm, 34.5 isohaline [21].

According to [17] and [27], Indonesian archipelago is the only region near the equator that connects two major oceans, the Pacific and Indian Oceans. This complicates the variability of ocean dynamics in the region, along with its complex topography, coastlines' geometry, and monsoonal winds. These factors may as well affect oceanography phenomena happening in the area. There are several known and indicated upwelling area in Indonesia, such as in southern Makassar Strait [5,7,18,21,22], in southern coast of Java and Sumatera [8,9], in Banda Sea [10,23], and in Timor Sea [11,12], as well as in Banggai waters in western Maluku Sea [4].

Maluku Sea located in the eastern Sulawesi Island and bordered with North Maluku Islands to the east. The deepest depth of Maluku Sea reaches 4,500 m, in contrast with shallow coastal water of Banggai Islands on its southwestern boundary, and opened passage to the Seram-Banda Sea in the southern boundary. There is still limited research on upwelling in Maluku Sea. There are SST cooling and chl-a blooming in Gulf of Tomini, affected by strong winds passing Maluku Sea, which is in good agreement with [4,13]. However, previous upwelling studies in this region have only provided a simplified physical mechanism analysis and only focused on surface features of upwelling. The objective of this study is to investigate physical processes and dynamics of upwelling, particularly changes in ocean-atmosphere variables before-during-after upwelling, mechanism of upwelling generating force during 2015 super El Nino event, and to analysis interannual variation of upwelling intensity related to ENSO between 2008-2015.

2. Methods

2.1. Study area

Study area is located off northeast Banggai waters in western Maluku Sea (figure 1). The southern boundary located in a shallow passage between Banggai and Taliabu Islands, connecting directly to northwestern Banda Sea. The eastern boundary is central deep (>2000 m) Maluku Sea, while western and northern boundaries are linked with outer Tomini Gulf and Gorontalo Sulawesi mainland. Peleng Strait is a narrow and shallow strait, located just in the northern Banggai Islands.

The sampling box (black rectangle) denotes for extraction of model/data validation. Black line represents *Hovmoller* analysis of ocean-atmosphere parameters. Yellow-line represents cross-section for seawater temperature, while red line indicates cross-section for transport-volume calculation. The daily time-series data analysis of model output and satellite imagery data comprised from 1 January to 31 December 2015, and interannual data analysis spanned from 2008 to 2015.

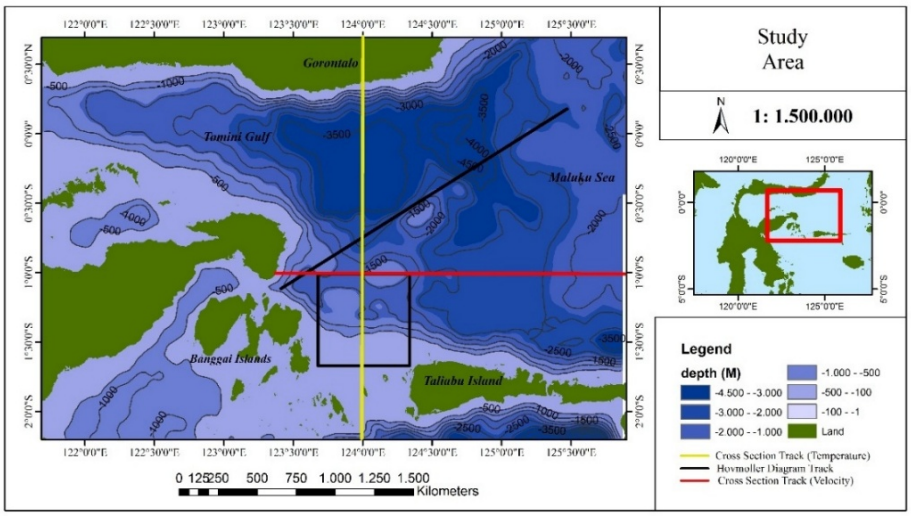

Figure 1. Study area off Banggai waters in western Maluku Sea.

2.2. The data

This study used several keys atmospheric and oceanic variables derived from satellite observation and INDESO model output. Those are sea surface temperature (SST), seawater temperature, wind speed, zonal and meridional wind stress components, latent heat flux, sensible heat flux, infrared heat flux, relative humidity, air temperature, instantaneous SST, salinity, and zonal and meridional current components. Model seawater temperature, salinity, and current are 3-dimensional data sets. These data acquired from the INDESO model. Configuration of this model described in detail [17]. Briefly, this model is based on NEMO (Nucleus for European Modeling of the Ocean) 9.0 [14] with 1/12° horizontal resolution. The horizontal grid is an extraction of global ORCA (global tripolar grid used in NEMO) grid at 1/12° developed at Mercator Ocean. The vertical grid spreads over 50 depth levels that a depth-dependent resolution (1 m at surface to 450 m near the bottom). Atmospheric forcing fields acquired from European Centre for Medium-Range Weather Forecasts (ECMWF).

Data accuracy of INDESO model output are validated using satellite imagery data. Satellite derived SST and chl-a data are used to map spatial distribution of upwelling indicated area. Satellite sea surface height anomaly (SSHA) and SST data were used to validate INDESO model output. The SSHA data with horizontal resolution of 1/4° or 27-28 km were obtained from the Copernicus Marine Environment Monitoring Service (http://marine.copernicus.eu/). The data based on assimilated multi-satellite data, such as Jason-3, Jason-2, and Cyrosat-2.

The SST and surface chl-a data are used to map spatial distribution data, were obtained from http://www.indeso.web.id/indeso_wp/index.php as remote sensing observation data of INDESO Project. SST data are derived from MODIS/AQUA and MODIS/TERRA satellite with horizontal resolution of 0.02°. Surface chl-a data are derived from Suomi-NPP satellite using VIIRS sensor with spatial resolution of 0.02°.

2.3. Data analysis

Data analysis of upwelling ocean-atmosphere variables follows procedure of time-series analysis methods [15]. Model outputs are validated using satellite data to estimate its accuracy. Both satellite observation data and INDESO model outputs reanalyzed and visualized. We computed and visualized monthly mean along the 2015 year to map the spatial evolution of upwelling from satellite imagery data. Model outputs reanalyzed to understand a mechanism of generating force of upwelling, to estimate transport volume, and fluctuation of atmospheric and oceanic variables. To analyze generating force of upwelling, winds fields and currents fields are visualized as monthly average. Transport volume estimation was calculated following [18]. The depth and area of upwelling are analyzed with vertical

structure of meridional current component, leading to estimate upwelling transport volume. We analyzed and visualized fluctuation of atmospheric and oceanic variables were *Hovmoller* diagram throughout 2015. Time-series ocean-atmosphere data are extracted from sampling box (figure 1) from 2008-2015 to analyses interannual variation of the variables related to El Nino Southern Oscillation (ENSO). The comprehensive analysis on physical processes and dynamics of upwelling and its variability related to ENSO in western Maluku Sea used various methods.

2.4. Data validation

INDESO model outputs were validated using satellite data, by comparing sea surface height model with observed sea level anomaly and sea surface temperature with observed SST retrieved from Copernicus, Marine Environment Monitoring Service. The plotting data along 2015 within a sampling box area used for validation, as shown in figure 1. Correlation coefficient determine the degree to which two variables are significantly correlated [15].

Sea level anomaly from both data shows the maxima during peak of the Northwest Monsoon (NWM) period (January-February), which decreases gradually from the first Monsoon Break (MB1), from March to June. While the minima occur during the Southeast Monsoon (SEM) period (June-August) (figure 2). Amplitude of fluctuations reveals that sea level anomaly is high during the NWM period and is remarkably low during the SEM period, with much higher frequency fluctuation appeared in the model due to higher temporal resolution. Correlation coefficient between model and observed SSHA is highly good (0.8713). Comparison of model and observed SST data is significantly high (0.9149) (figure 3). Both data-series show similar fluctuation pattern throughout the year. According to [15], both values show that accuracy of model is pretty good agreement and highly correlated with the data. Thus, INDESO model depicts observed condition and the model data sets are suitable for further analysis.

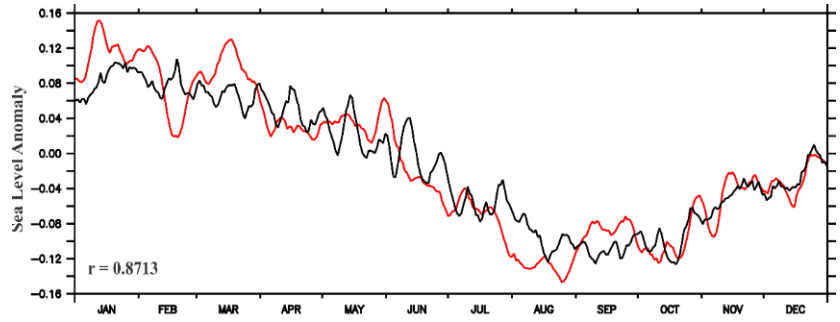

Figure 2. Comparison between INDESO model sea surface height anomaly (black line) and observed satellite data (red line) in 2015. Correlation coefficient between the data is 0.8713.

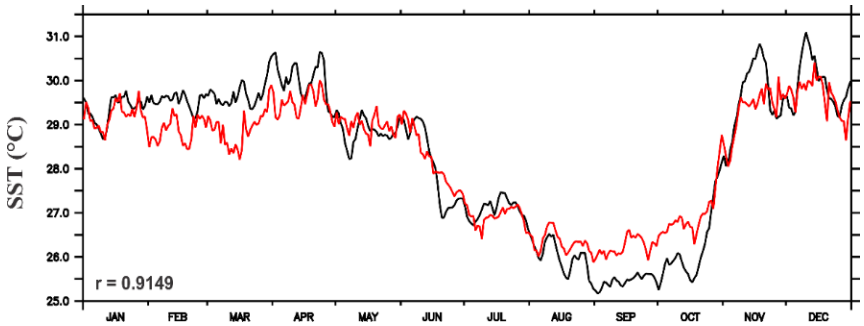

Figure 3. Comparison between sea surface temperature (black line) model and observed satellite data (red line) in 2015. Correlation coefficient is 0.9149.

3. Results and discussion

3.1. Surface features of upwelling

The first step to inspect upwelling event in the study area is from monthly mean SST and chl-a data from satellite imagery data. It reveals SST cooling and chl-a blooming related to upwelling that occurs during the SEM period from June to October 2015 (figure 4 and 5).

The SST during January-June varies from 27-31°C, with lower temperature is mostly seen in the southwestern region, close to central Sulawesi. In January, highest temperature can be seen around Banggai Island. Later in February and March, the SST distribution is similar, which shows much warmer water in the western part, while cooler water is seen in the northeastern region and closed to Taliabu Island (figure 4). As in May begins, marking the end of the MB1 period, SST starts to decrease, which vary from 27.4-30.4°C. Much cooler water is seen between Banggai and Taliabu waters with temperature of 27. 4 °C. This area of low SST evolves larger in June, the beginning of the SEM period, with SST ranges from 26.5-29.5°C. Low SST is distributed in most part of the region, except in Tomini Gulf. The lowest SST is found in between Banggai and Taliabu waters.

Contrast to first half of 2015, SST during the second half is lower, as shown cyan color dominated with hints of green and yellow, which ranges from 26-30°C. Highest temperature area can be seen around Tomini Gulf waters, while SST of Maluku Sea only reaches 27°C at most. High SST can be affected by region characteristics, as Tomini Gulf is semi enclosed waters (figure 4).

Low SST appears in the southern region, a pathway of water mass intrusion from northwestern Banda Sea. SST gradually increase towards the north, which changes to northeast direction near northern Gorontalo Sulawesi mainland (see figure 1). SST is generally minimum during the SEM period. Drastic changes appear during the SEM period which only reaches 26.2°C at most. Largest low SST can be seen in September, which then slightly weaken in October. This pattern changes drastically in November and December, which shows the lowest value of 28°C (figure 4).

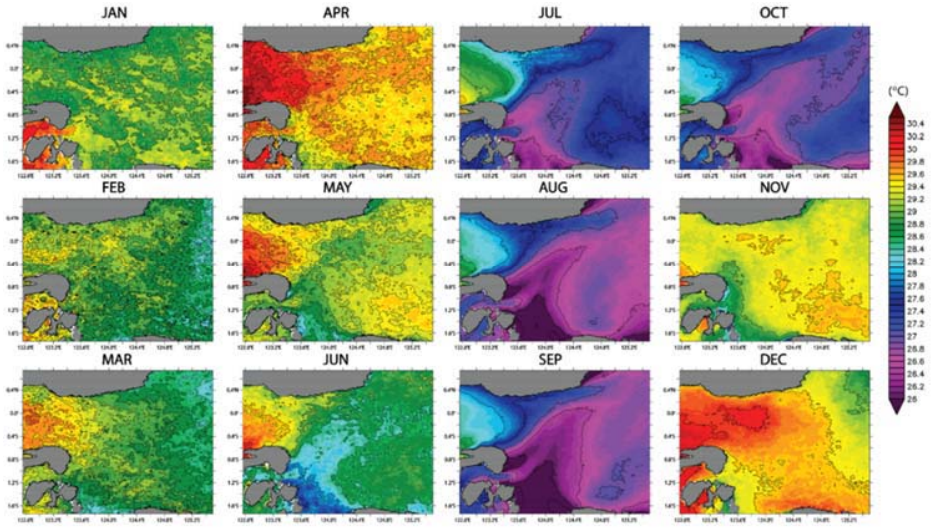

Figure 4. Evolution of monthly sea surface temperature in 2015, indicating surface features of upwelling off Banggai waters in Maluku Sea during the SEM period (June-October).

Chlorophyll-a (chl-a) in Maluku sea waters ranges from 0.02 – 12.1 mg/m^3 along 2015. High chl-a can be found in coastal area, which may be related to nutrient input from land which affects primary productivity. During the NWM period, surface chl-a ranges from 0.02 – 0.98 mg/ m^3, the highest chl-a exists in coastal area, while in Maluku Sea only reaches 0.68 mg/ m^3 with similar the coastal area (figure 5). It is in good agreement with [4], reporting that the chl-a in Maluku Sea ranges from 0.1 – 1.1 mg/ m^3 during the NWM period.

From January to April, there is no significant changes in spatial distribution of chl-a. But as the MB1 ends in May, high chl-a is found not only in coastal area but also off the Banggai waters. Tip of Tomini Gulf and Banggai waters and Taliabu waters reveal higher chl-a. It evolves into bigger area in June, which is shown by larger area (in green), which represents higher compared to its surroundings. The spatial distribution shows similar pattern with SST cooling (figure 5).

An increase of chl-a continues during the SEM period, reaching 0.98 mg/m^3 and above, with the highest chl-a is seen around Banggai Island and its eastern region. Area with high chl-a enlarges, evolve in northeast direction to northern Sulawesi, with the lower chl-a is seen in Peleng Strait, just north of Banggai Island.

Large seasonal variation of SST and chl-a in Maluku Sea is consistent with previous study e.g. [4]. Seasonal peaks of chlorophyll-a blooming and SST cooling in Maluku Sea happens in August [13]. High chl-a is gradually decreasing in October, and can no longer be seen in November and December, with chl-a only reaches 0.32 mg/m^3.

Past study (e.g. [4]) proposed that mechanism regarding chl-a blooms in Maluku Sea is associated with increased alongshore wind fields that drag cold water from beneath mixed layer, which support to phytoplankton growth in the region. Following section, we discussed more detail seasonal changes of surface wind fields and near-surface current in the region related to upwelling event.

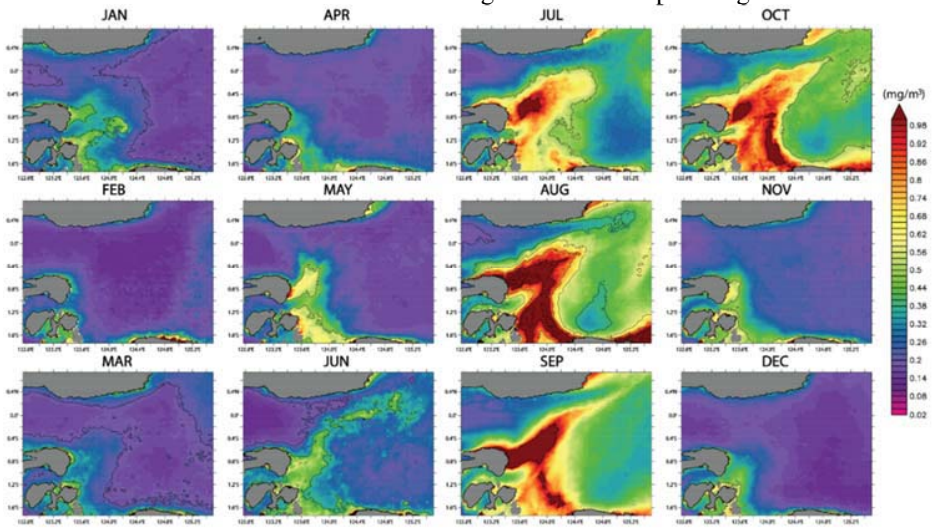

Figure 5. Evolution of monthly surface chl-a concentration in 2015 that indicates the upwelling features during the SEM period in Banggai waters in Maluku Sea.

3.2. Generating mechanism of upwelling in Banggai waters

Monthly mean of wind stress distribution is shown in figure 6. The arrows represent wind stress vectors, and its length represents wind stress magnitude. Spatial distribution of wind stress magnitude is also shown, ranging from 0 to 0.06 N/m^2.

During the NWM period, intensity of wind stress is rather high. During the first three months, northwesterly and northerly wind fields blow from Tomini Gulf and Maluku Sea to Banda Sea, which weaken as the MB1 period begins in March. In April, wind stress significantly weakens, as seen on the figure 6, the color shown in April is different, and wind stress only reaches 0.008 N/m^2. As May begins, southerly reversal wind stress occurs Banda Sea, heading northern Sulawesi. The wind fields intensify in June, and get much stronger when the SEM period begins, with wind stress reaching 0.048 N/m^2.

During the SEM period southerly monsoonal wind stress fields are fully excited. Wind stress with highest intensity tend to come from Banda Sea, which then head to Tomini Gulf and Maluku Sea. This high intensity wind stress reaches its peak in August. In September and October, wind stress gradually weakens, while in November it reaches almost calm over the region, as shown with significant changes of color, with wind stress only reaches 0.008 N/m^2. As the NWM period begins in December, the

northerly-northwesterly wind fields appear with only 0.032 N/m^2, heading to Banda Sea from Maluku Sea and Tomini Gulf.

Wind stress gradually increase of wind stress from June to August, as the southerly monsoon winds begin to intensify in July. This strong alongshore wind stress exceeding 0.06 N/m^2 is clearly seen from the passage between Banggai and Taliabu Islands, to the tip of Tomini Gulf, causing SST to drop by 2^{o}C and increasing the surface chlorophyll-a of about 0.7 mg/m^3(figure 6). This pattern is related to the changes of SST distribution in the study area. SST shows significant decrease during the SEM period, which can be seen in the area between Banggai and Taliabu Island to its north, until the mouth of Tomini Gulf. Area with low SST widens to the northeastern waters.

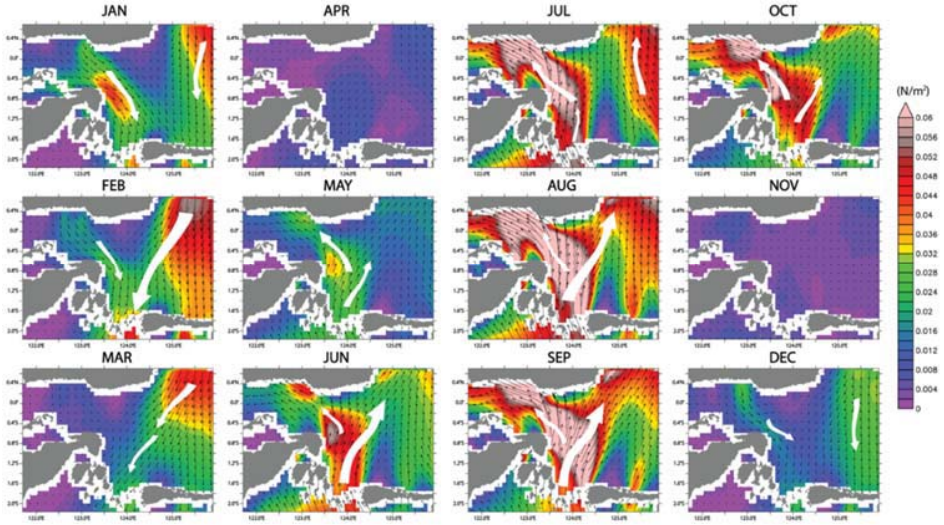

Figure 6. Evolution of monthly mean wind stress vectors in 2015.

Normal Ekman upwelling event tends to be affected by Coriolis effect, deflecting surface currents from wind direction, to the right of the wind direction in the northern hemisphere, and to the left in the southern hemisphere. Following Ekman theory, Ekman transport due to wind stress drag, net water movement is directed perpendicular to wind direction, to the left of the wind stress in southern hemisphere and to the right in the northern hemisphere [2]. The illustration of upwelling mechanism can be seen in figure 7.

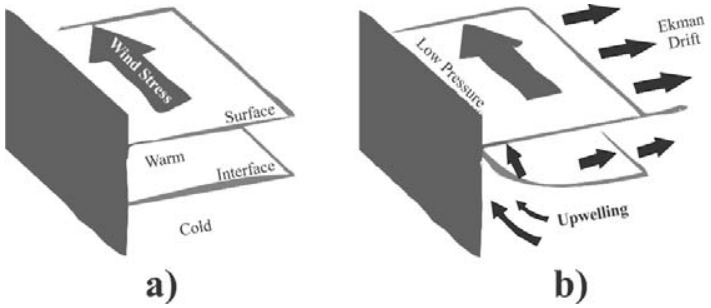

Figure 7. Schematic Ekman upwelling, (a) initial condition and (b) upwelling condition. In northern hemisphere, southerly winds stress result Ekman drift (transport) to the right of the wind direction. (after [2]).

Upwelling area in western Maluku Sea lies from the shallow passage between Banggai and Taliabu Islands to its northern waters. If we consider the Ekman theory with included Coriolis Effect in southern hemisphere, the Ekman transport due to southerly winds must be directed westward. However, Ekman drift in this study area is directed northward rather than westward. Since the study area is closed to the

equator (2°S - 0.5°N), then the Coriolis Effect can be neglected. This implies that strong persistent southerly monsoonal winds fields during the SEM period drag directly surface water quasi-northward. Shallow passage between Banggai and Taliabu Islands is the initial path of colder water mass flow. Through the mechanism of wind-driven coastal upwelling by neglecting Coriolis Effect, surface water mass is dragged by the wind directly northward. The vacant surface water column is then replaced by colder water mass from deeper layer. Due to the boundary of Gorontalo Sulawesi mainland, the flow direction then changes to the northeast. During the MB2 in October and November, the wind stress weakens and upwelling event can no longer be seen, as seen from appearance of warmer SST and low surface chl-a in the southern area.

3.3. Near-surface circulation

As the wind stress alters the surface layer, surface current is established in upper-layer which is similar to the monsoonal wind field direction (figure 8). During the NWM period, surface circulation flows southward, though current vectors heading northeast can also be seen. It may be affected by secondary ITF Maluku pathway which recirculates in eastern part of Maluku Sea. Similar pattern can be seen during the MB1 period with lower magnitude. At the end of the MB1 period, sea surface temperature and surface circulation change and start flowing southward.

Entering the SEM period, the northward flow from northwestern Banda Sea can be seen in the passage between Banggai and Taliabu Islands. Strong northward currents from Banda Sea is associated with a development of colder STT. Spatial distribution of low SST also develops to the north direction. Surface current in the near-surface layer is directly affected by wind fields. The model shows no deflection on current direction relative to the wind, since Coriolis Effect vanishes in the equator area.

Due to this reason, current vectors during the SEM period flows quasi-northward. Shallow water between Banggai Islands and Taliabu Island as the pathway eases dragging of water mass. Strong southeast monsoonal wind generates stress on the surface. This causes dragging of water mass to certain water depth, and due to non-existent Coriolis' effect, water mass is dragged straight to the north, causing water masses on shallower area replaced by colder deeper water mass, commonly known as upwelling (figure 8).

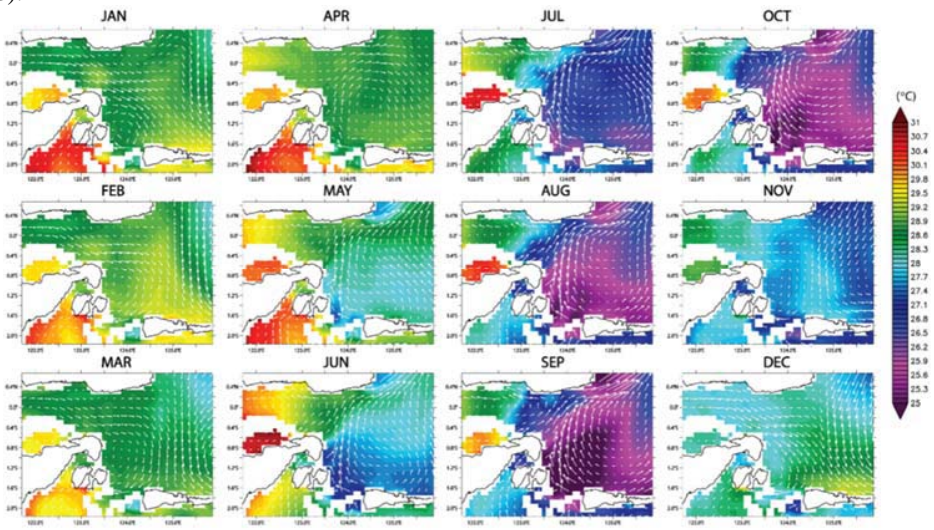

Figure 8. Monthly mean of model current vectors in 25 m depth and its seawater temperature in 2015

Vertical extent of seawater temperature and meridional current component during the NWM and SEM periods are shown in figure 9 and figure 10. It is seen clearly that near-surface warmer water with temperature above 28°C is found during the NWM period, in contrast to that the SEM period in which colder water above 24 °C is predominant. So that, temperature difference between two monsoon period is about 2 °C (figure 9). In general, seawater temperature ranges between 10 and 31°C during the NWM. During the SEM period, seawater temperature reaches 10°C in deeper layer, but the upper layer has

lower temperature compared to the NWM period. Highest temperature only reaches 28°C, and can be seen along the track. In mixed layer, the temperature difference reach 2°C cooler during the SEM period, while in deeper layer, temperature difference is quite small. This suits the spatial distribution of SST, which lower during the SEM period, and evolve from southern boundary, in shallow passage between Banggai and Taliabu Islands towards the north. As seen in figure.9, isotherm of 26 °C is outcropped to surface layer during the SEM "upwelling" period. Coldest water with temperature 25-26 °C can be seen along 1.8°S to 1°S. This is the center of upwelling in Banggai waters. Colder surface water is developed due to upwelled water from deeper layer. During the NWM period isotherm of 26 °C lies at 80 m depth, but it uplifts to surface layer during the SEM "upwelling" period (figure 9).

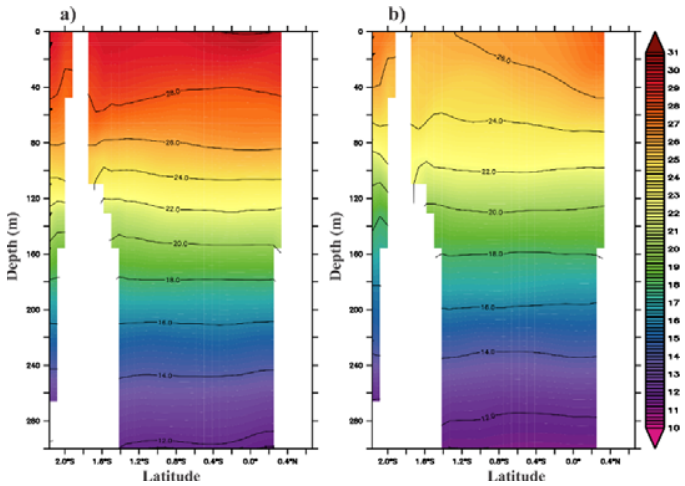

Figure 9. Vertical section of seawater temperature along 124°E (a) during the NMW period in February, and (b)during the SEM period in August 2015. Upwelling is indicated by outcropped isotherm of 26°C to the sea surface (b).

Vertical section of meridional current component during different monsoon period shows large seasonal variation of northward surface flow associated with upwelling event. During the NWM period, strong southward flow near surface layer is found (figure 10a), but closed to coastal area reveals weak northward flow. However, during the SEM period along with the occurrence of upwelling event, much stronger northward flow occurs (figure 10b). This northward current transports COLDER surface water mass from the center of upwelling in the shallow passage between Banggai and Taliabu Islands.

Vertical distribution of meridional current component varies with depth, which much stronger at the surface and much weaker at deeper depth. During the NWM period (represented by February), meridional velocity component reaches above 0.5 m/s that flows southward in surface layer and quasi-vanishes at deeper depth (figure 10a). During the SEM period (August), meridional velocity component reaches 0.78 m/s northward in surface layer and weakens at 80 m depth. At deeper depth (e.g. 160 m depth) meridional velocity component southward is seen, exceeding magnitude of 0.3 m/s.

Upwelling event in Banggai waters indicated chl-a blooming and SST cooling, along with much stronger southerly wind stress and northward surface current. The upwelling appears during the SEM period, commenced in June and terminated in October with its peak in August. During the peak of upwelling in August, isotherm of 26 is outcropped at the sea surface, and seawater temperature drops to about 2 °C, compared to that the NWM period. Vertical extent of upwelling depth is estimated to about 60 m depth. Upwelling indicated region is shown by the area marked by red square (figure 10b), which shows strong northward flow. This region reaches about 60 m deep, with area approximately 6.72 km^2. From this area, transport volume estimation can be known, with the value of 0.4 Sv. Intensity of transport volume of upwelling water mass may differ from area to area, depending on magnitude of the current, and transport calculation approach. One of the external factors may contribute to upwelling in Maluku

Sea is associated with interannual climate anomaly of El-Nino Southern Oscillation (ENSO), where Maluku Sea showed significant correlation with ENSO [5].

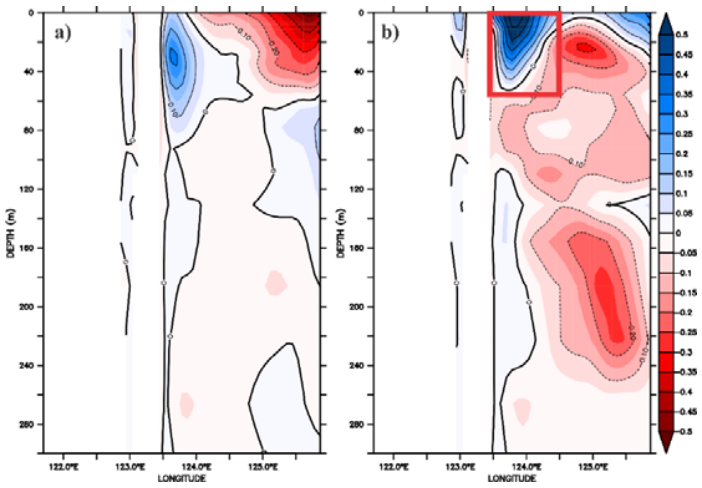

Figure 10. Vertical section of meridional current component in February (a) and August (b) 2015. Note: red rectangle denotes upwelling extent during the SEM period.

3.4. Evolution of ocean-atmosphere changes related to upwelling episode

Heat fluxes and instantaneous SST changed during the SEM "upwelling" period. While instantaneous SST cools, latent heat flux increases. Infrared heat flux weakens during the SEM period and no significant changes can be seen in relative humidity (not shown). Heat flux intensification may lead to heat loss in the mixed layer of atmosphere, and when heat loss exceeds, air temperature decreases. This may explain the relation between increased sensible heat flux intensification and decreased air temperature. Wind stress intensification may also affect heat flux intensification [16].

Strong seasonal variation is found from the ocean-atmosphere variables, contrasting between two monsoon periods. During the SEM period, modulus of wind speed is strongest, coincides with wind stress. Compared to zonal wind stress component, meridional wind stress component is significantly stronger. Air temperature cools during the SEM period. According to [16], wind stress intensification may affect heat flux intensification. Heat flux intensification may lead to heat loss in the mixed layer of atmosphere, and when heat loss is bigger than heat gain, temperature will be lower. This explains the changes of sensible heat flux that intensifies while air temperature is cooling.

Stronger wind stress drags surface water masses northward, which replaced by colder water mass from water column, generally known as upwelling. While simultaneously, wind stress is also affecting heat flux and heat loss in the study area, which explains low air temperature (not shown).

Time-series of ocean-atmosphere variables, extracted from a rectangle sampling box in figure 1, is shown in figure 11. Rapid inspection from the series revealed that negative anomaly of SST is commenced from June to October 2015. This seasonal change of SST is consistent with others variables (figure 11), suggesting that upwelling onset begins in June and is terminated in October. Upwelling affects on altering water mass as response to water mass uplifting, along with changes on atmospheric variables. Large seasonal fluctuation is found from the series. SST is minimum in June, then increased gradually in October. Contrary to SST, chl-a increased during the same period in the year. It increased significantly during June-October, as it reached maxima of 12.1 mg/m^3. Ekman drift due to strong persistent southerly monsoon winds field during the SEM period plays a role as the uplifted colder water mass from deeper water column (60 m depth). From there, higher nutrient colder water contributed to higher primary productivity, hence higher chl-a.

As discussed previously, wind stress generated upwelling in the area. Upwelling area evolved northward from southern boundary of shallow passage between Banggai and Taliabu Islands. Thus,

fluctuation of meridional wind stress is examined (figure 11c). Started from June, meridional wind stress increased, reached its peak in September, and decreased again in October. Estimated transported volume of water mass also shows similar fluctuation (figure 11d). Northward transport (positive anomaly) appeared during the SEM period that transport surface water mass from southern boundary, while during the NWM period negative anomaly means southward transport volume. Much stronger southward transport is found in November-December 2015.

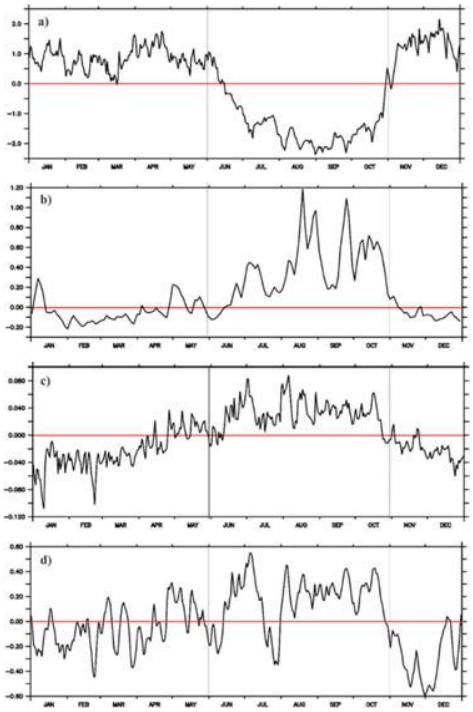

Figure 11. Anomaly of a) SST, b) chlorophyll-a, c) meridional wind stress, and d) transport volume estimate in 2015

Seasonal variation of atmospheric variables is also found (figure 12). Infrared heat flux and air temperature are minima during the SEM period, while sensible heat flux increases. This changes may occur due to heat loss, as heat flux intensifies when wind stress intensifies (figure 12). This is consistent with increased meridional wind stress during the SEM (figure 11).

As the atmospheric characteristics are changing, the changes on water mass also occur. Northward transport volume is higher during the SEM period, resulting in changes of sea surface temperature and chlorophyll-a (figure 11).

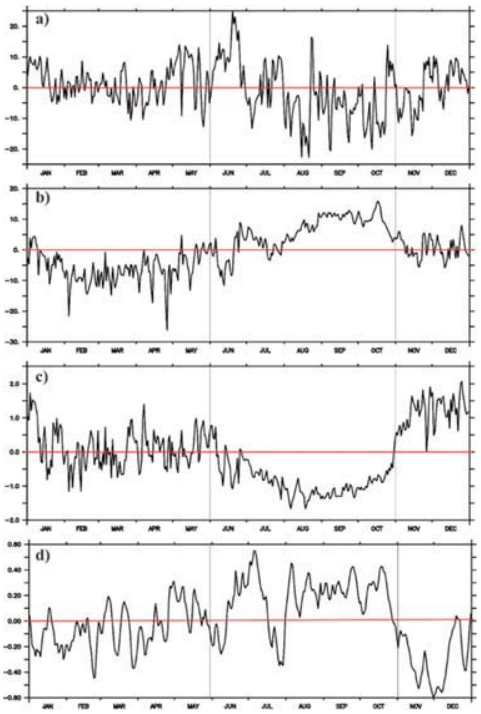

Figure 12. Anomaly plot of a) infrared heat flux, b) sensible heat flux, c) air temperature, and d) transport volume estimate in 2015

Seasonal fluctuation as mentioned above, can be seen as the effect of upwelling. Wind stress generates the upwelling in Maluku Sea, and induced the changes on oceanic and atmospheric variables. Initial condition before onset of upwelling, strong persistent southerly wind induced surface flow northward. This then generated the water mass transport. The initial upwelling pathway in shallow passage between Banggai and Taliabu Islands, possessed vacant surface layer due to transported water mass. This leads uplifting deeper colder water mass to replace the warmer surface transported water, which caused SST cooling in certain area, as shown with blue, includes the waters between Banggai and Taliabu Islands, to the tip of Tomini Gulf (figure 13).

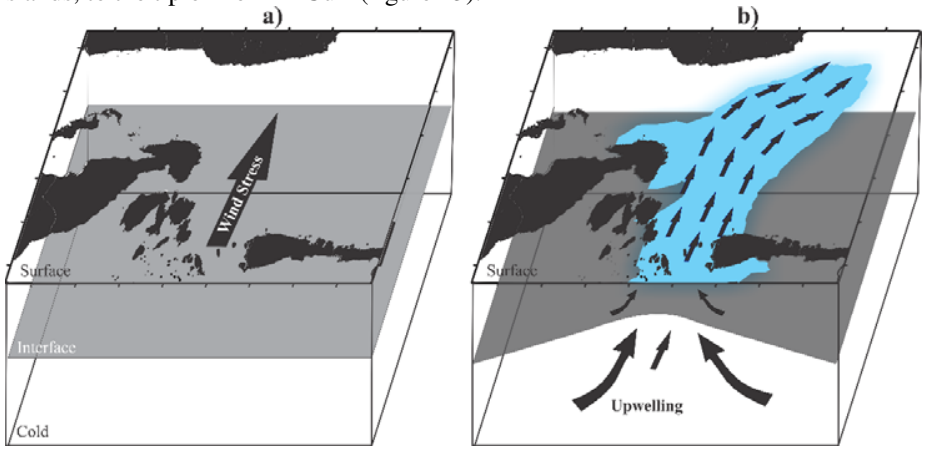

Figure 13. Schematic of upwelling process in Maluku Sea, a) initial condition and b) upwelling condition

The changes can also be seen quantitatively, as upwelling alters the condition of both oceanic and atmospheric parameters. As the upwelling onset in June begins, strong persistent southerly wind changes

the wind stress magnitude. From there, northward wind-driven surface current strengthens and leads to water mass transport. It then alters SST, which cools down, as well as chl-a blooms. In addition to that, atmospheric variables also alter. These upwelling characteristics can be summarized in table 1 below.

Table 1. Characteristics of ocean-atmosphere variables during upwelling period in 2015.

Ocean-Atmosphere variables	Range (2015)	Range (Jun-Oct 2015) during upwelling period
SST (°C)	26 – 31	26 – 28
Chlorophyll-a (mg/m^3)	0.02 – 12.10	0.98 – 12.10
Wind Stress ((N/m^2)	0 – 0.06	0.032 – 0.060
Air Temperature (°C)	25.3 – 29.5	25.3 – 27.0
Sensible Heat Flux (W/m^2)	-42 – 10	-6 – 10

A proposed mechanism of upwelling in Maluku Sea is induced by southerly winds passing through Maluku Sea during the SEM period (figure 14). Wind stress shows that there is strong southerly wind blow during the SEM period. The wind stress generates wind-driven upwelling in western Maluku Sea. SST cooling and chl-a blooming are induced by the mechanism of wind-driven upwelling, the alongshore wind may drag the cold water from beneath the mixed layer to the surface in the Banggai tip waters, and from there, support phytoplankton growth in the region [4].

Wind intensification caused much stronger wind stress, affecting released heat flux. This causes an increase on seawater density, thus water mass sinks. In addition, the wind stress affects surface current in the mixed layer, dragging surface water mass northward. This is proposed mechanism of upwelling in Maluku Sea.

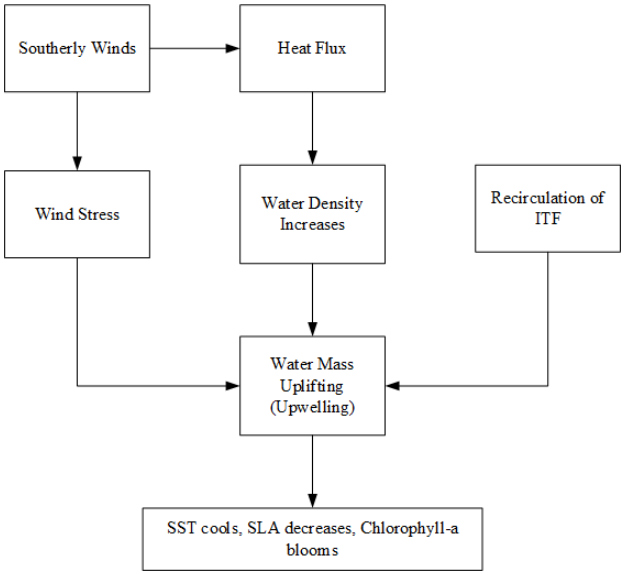

Figure 14. Proposed mechanism of upwelling of Banggai waters in Maluku Sea.

In the northern part of study area, recirculation of ITF Maluku plays a role on upwelling intensity during the SEM period. The existence of ITF's second pathway and Gorontalo Sulawesi mainland shape deflected upwelling area to the northeast. From the tip of Tomini Gulf, the upwelling area evolves toward

northeast as Sulawesi mainland acts as solid boundary, as well as recirculation of ITF on the northeastern part of study area. Upwelling then causes SST cooling, decreasing sea level, as well as chl-a blooming.

3.5. Interannual variation of upwelling intensity related to ENSO

Analysis of monthly mean of satellite imagery and model output data sets in 2015 revealed clearly upwelling event off Banggai waters in Maluku Sea. Upwelling mechanism is mostly forced by the strong persistent southerly monsoon winds during the SEM period. Furthermore, initial upwelling region is located in southern boundary of a shallow passage between Banggai and Taliabu Islands, where it is directly linked with northwestern Banda Sea. It is found that upwelling event is commenced in June with its peak in August and is terminated in October. Ocean response to the upwelling processing is upwelled seawater temperature cooling with outcropped isotherm of 26 to the sea surface, chl-a blooming, and increased near-surface northward transport volume. These ocean responses propagate northward from initial upwelling area in the southern boundary. Meridional wind stress and current components show similar evolution.

In term of interannual variability, it is interesting to examine upwelling intensity during the 2015 upwelling event in Maluku Sea and to compare with past years of upwelling intensity, since the occurrence of 2015 upwelling event was coincident with the interannual climate anomaly of El Nino Southern Oscillation (ENSO) 2015/16. The 2015/2016 El Nino event is one of the strongest on record, comparable to the 1982-1983 and 1997-1998 events that triggered widespread ecosystem change in the northeast Pacific [23]. The 2015-2016 El Nino event is categorized as super El Nino [24]. Upwelling intensity along the southern Java Sumatera waters was found much stronger during the El Nino year [8]. However, study of interannual variation of upwelling in interior Indonesian seas, such as in Banggai waters Maluku Sea, needs to be advanced.

Time series of standardized southern oscillation index (SOI) obtained from [22], shows ENSO events that appeared between 2008-2015 (figure 15a). Positive anomaly (red) of the SOI represents La Nina events, while negative anomaly (blue) is for El Nino events. The ENSO events are defined if the index anomaly exceeds ±2. Over that period, there are weak La Nina 2008/2009, strong La Nina 2010/2011, and weak El Nino 2009/2010 and strong El Nino 2014/2015.

Time series of anomaly of ocean-atmosphere variables (extracted from sampling box in figure 1) between 2008 and 2015 is shown in figure 15(b-g). It is apparent that the variables indicate interannual variability related to ENSO (figure 15a), which show two major events, La Nina 2010/2011 and El-Nino 2014/2015. Peak of La Nina can be seen in 2010 while El Nino in 2015. Anomaly of ocean-atmosphere variables present on figure 15(b-g), with annual mean removed to seek better understanding on interannual variability.

The ocean-atmosphere variables show interannual variability, in which SST, SSH, and seawater temperature are well positive correlated, while meridional wind stress, salinity (0-25 m), and meridional current (0-25 m) are well negative correlated with SOI indices. Meridional wind stress (figure 15b) exhibits positive (negative) anomaly during El Nino (La Nina). The positive anomaly during El Nino 2015 is not as significant as the negative anomaly during 2010 La Nina, but it changes to great negative anomaly during the end of El Nino 2015. SST shows different anomaly during La Nina and El Nino. During El Nino (La Nina) event, negative (positive) anomaly of SST occurs, with SST anomaly significantly increased as El Nino 2015 ends. Similar event shown in figure 15d of SSH, where negative (positive) anomaly can be seen during El Nino (La Nina), with more significant anomaly changes seen during El Nino 2015.

Aside from the surface variables, oceanic parameters in the mixed layer alters as well. According to [13], ENSO modified the upwelling's magnitude in Maluku Sea. The western Pacific surface temperature plays role on controlling monsoon, with higher (lower) surface temperatures during La Nina (El Nino) years, leading to stronger monsoon [19]. Stronger southeast monsoon then leads to stronger southerly winds in the study area. This southerly winds impact on enhanced (reduced) the wind stress during El Nino (La Nina), shown by positive anomaly of meridional wind stress. Thus, alters the SST and SSH anomaly as well. The enhanced upwelling intensity during El Nino is indicated by the anomaly on mixed layer (figure 15d-g).

During the El Nino (La Nina) event, negative (positive) anomaly of seawater temperature (0-25 m) occurs. Greater anomaly can be seen during El Nino 2015. On contrary, salinity on the upper 25 m depth displays positive anomaly during El Nino. The increased southerly meridional wind stress during El Nino generates greater northward meridional current, shown by positive anomaly during El Nino 2015, which is much stronger in comparison with negative anomaly during La Nina. The greater meridional current drags surface water mass, letting a vacant area on the surface then filled with water mass from deeper colder water mass. The latter water mass has different characteristics, hence the increase of salinity and seawater temperature on the upper 25 m depth during El Nino.

Figure 16 summarizes interannual variation of ocean-atmosphere variables, related to upwelling intensity, during each upwelling period from 2008-2015. In general, figure 16a shows similar variability throughout 2008-2015, where positive anomaly of each variables can be seen during 2010 La Nina event, while the strongest negative anomaly is seen during 2015 El Nino event. Less magnitude of change is found in air temperature, while the other three variables do not differ as much. Changes on SST as well as seawater temperature in mixed layer (T25m and T50m) are bigger as it is directly affected by the uplifting water mass during upwelling.

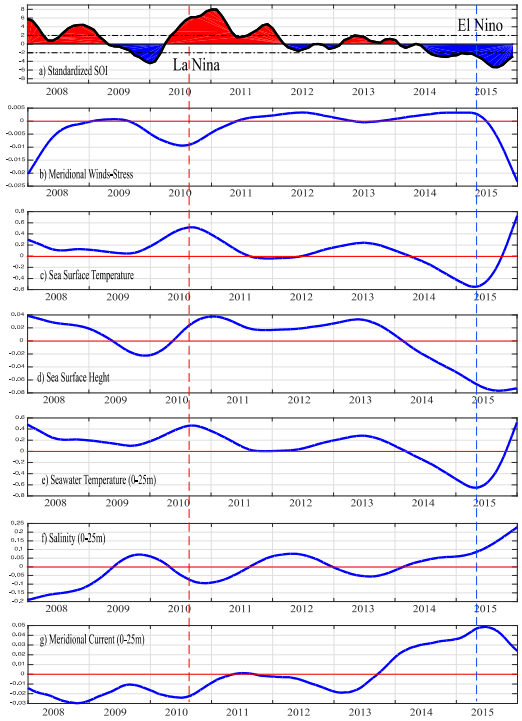

Figure 15. Time-series of ENSO indices (represented by SOI indices, a) and anomaly of ocean-atmosphere variables (b-g) in Banggai upwelling area in Maluku Sea. Note: daily ocean-atmosphere variables (b-g) are removed annual mean.

During the 2015 El Nino event positive anomaly of meridional wind stress is found, which is similar to that meridional current component in the upper 25 m depth (V25m) (figure 16b). During 2010 La Nina event, the zonal current component reaches positive anomaly while the others have the strong negative anomaly. For the meridional current component, it shows strong positive anomaly during 2015 El Nino event and significantly differs from the other three variables. This may occur due to enhanced upwelling intensity as impacted by El Nino event.

Table 2 summarizes anomaly of ocean-atmosphere variables during upwelling period (averaged between June-October) for each each year. Upwelling intensity (UI) is also shown in the last column, which is defined as the sum of anomaly of 9 ocean-atmosphere variables. As discussed previously,

anomaly of ocean-atmosphere variables between 2008-2015 differs significantly during 2 specific periods: 2010 La Nina and 2015 El Nino events (figure 15 and 16). Meridional wind component acts as the local forcing of the upwelling, which was very weak during La Nina event, while the strongest value can be seen during El Nino event. This leads to much stronger meridional current component in the upper 25 m depth as well. Direction of meridional component flow southward during La Nina event, and in contrast, flows northward with much stronger value during El Nino 2015.

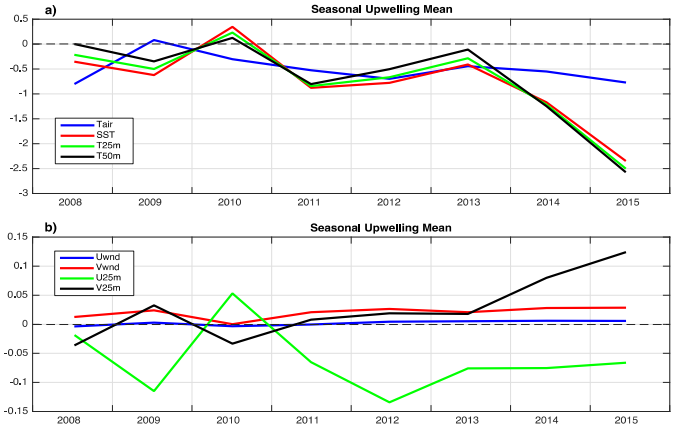

Figure 16. Interannual fluctuation of ocean-atmosphere variables in the upwelling region (off Banggai waters) between 2008 and 2015. The variables are averaged from June to October, representing upwelling intensity for each upwelling period; (a) air temperature (Tair), sea surface temperature (SST), seawater temperature 0-25m (T25m), seawater temperature 0-50m (T50m); (b) zonal wind component (Uwnd), meridional wind component (Vwnd), zonal current component 0-25 m (U25m), and meridional current component 0-25m (V25m).

Finally, it is evident that on interannual time-scale, fluctuation of upwelling intensity (UI) in Banggai waters exhibits positive anomaly (+0.27) during 2010 La Nina event, in contrast to 2015 super El Nino with the strongest negative anomaly of UI (-5.35) (table 2). Thus, it can be summarized that upwelling intensity during the super 2015 El Nino event is the most powerful upwelling intensity, compared to others ENSO events between 2008-2015. It is also shown that the weakest upwelling intensity is noted during the strong 2010 la Nina event. This suggests that upwelling intensity in Banggai waters are significantly impacted by external factors such as ENSO.

Table 2. Anomaly of ocean-atmosphere variables associated with *Upwelling Intensity* (UI). Each variable is averaged between June and October for each upwelling period.

Year	Tair	SST	SSH	uwind	vwind	T25m	S25m	U25m	V25m	Upwelling Intensity
2008	-0.791	-0.355	0.003	-0.003	0.013	-0.220	-0.019	-0.020	-0.035	-1.43
2009	0.082	-0.623	-0.040	0.003	0.024	-0.499	0.317	-0.115	0.033	-0.82
2010	-0.302	0.346	0.025	-0.003	0.001	0.231	-0.045	0.053	-0.033	+0.27
2011	-0.526	-0.877	-0.043	-0.009	0.021	-0.842	0.107	-0.065	0.008	-2.22
2012	-0.696	-0.779	-0.018	0.004	0.027	-0.665	0.238	-0.134	0.019	-2.00
2013	-0.443	-0.408	0.021	0.005	0.021	-0.284	0.051	-0.076	0.018	-1.10
2014	-0.550	-1.169	-0.072	0.006	0.028	-1.215	0.233	-0.075	0.080	-2.73
2015	-0.767	-2.335	-0.144	0.006	0.028	-2.486	0.291	-0.066	0.124	-5.35

4. Conclusion

From satellite imagery data, upwelling event is indicated by SST cooling in June in southern boundary where it extends northward, and terminates in October. The lowest SST (<26°C) is found in September. The cooling episode is followed by chl-a blooming one-month later from July to October. Concentration of surface chl-a reaches its maximum in August (>1 mg/m^3). Generating mechanism of upwelling in the study area is forced by strong and persistent southerly monsoon winds stress that exists from June to October during the Southeast monsoon (SEM) period. Following upwelling theory, in high-latitude southern hemisphere, southerly winds stress drag surface water northward and Ekman drift deflected to the left from the wind direction. However, since the study area is just over the equator, then the Coriolis effect may be neglected. So that the Ekman drift must be similar to the wind direction. This "special coastal-equator upwelling case" can be proven from surface circulation pattern, where the current vectors flow quasi-northward along the eastern Banggai Waters.

During upwelling episode, northward transport volume is drastically increased from surface to about 60 m depth. Shallow passage between Banggai and Taliabu Islands provides an initial upwelling region, where dragged warm surface water is replaced by upwelled colder water from sub-surface (80 m depth) layer. The upwelling area then evolves northward. Recirculation of Maluku ITF in southern boundary may contribute to the northward flow of upwelling. Vertical section of seawater temperature shows that during upwelling episode, isotherm of 26°C is outcropped to the sea surface. In contrary, during non-upwelling (the NWM period) this 26°C isotherm lies deeper at 80 m depth and temperature of 28-29°C is dominant at surface. Ocean-atmosphere variables changes in response to the upwelling event.

On interannual time-scale related to ENSO between 2008-2015, the most powerful upwelling intensity in Banggai waters was revealed during super El Nino 2015 with index of (-5.35), in contrast to weak upwelling intensity during strong La Nina 2010 (+0.27). Hence, Pacific origin of ENSO controls significantly on physical processes and dynamics of upwelling in the study area.

Acknowledgements

We would like to thank INDESO project Indonesia for providing and accessing to the model output data sets. We are indebted to CLS France, Mercator-Ocean, and Copernicus operational oceanography of Europe for providing satellite imagery data sets. We wish to thank Reviewer(s) for comments and critics to improve the manuscript.

References

[1] Duke D L and Sinz P D 2010 *Exact Solutions for Wind-Driven Coastal Upwelling and Downwelling Over Sloping Bathymetry* (California: California Polythecnic State University)
[2] Cushman-Roisin B and Beckers J 2011 *Introduction to geophysical fluid dynamics: physical and numerical aspects* Academic Press
[3] Habibi A, Setiawan R Y and Zuhdy A Y 2010 Wind-driven coastal upwelling along south of Sulawesi Island *Ilmu Kelautan* **15**(2) 115-118
[4] Setiawan R Y and Habibi A 2011 Satellite detection of summer chlorophyll-a bloom in the Gulf of Tomini *IEEE Journal of Selected Topics in Applied Earth Observations and Remote Sensing* **4**(4) 944-948
[5] Atmadipoera A S and Widyastuti P 2014 A numerical study of upwelling mechanism in Southern Makasssar Strait *JITKT* **6** 355-371
[6] Kemili P and Putri M P 2012 Pengaruh durasi dan intensitas upwelling berdasarkan anomali suhu permukaan laut terhadap variabilitas produktivitas primer di perairan Indonesia *JITKT* **4**(1) 66-79
[7] Nontji A 2007 *Laut Nusantara* (Jakarta: Djambatan)
[8] Susanto R D, Gordon A L and Zheng Q 2001 Upwelling along the coasts of Java and Sumatra and its relation to ENSO *Geophys. Res. Letters* **28**(8) 1599-1602
[9] Kuswardani R T D and Qiao F 2014 Influence of the Indonesian throughflow on the upwelling off the east coast of South Java *Chin. Sci. Bull.* **59**(33) 4516–4523

[10] Gordon A L and Susanto R D 2001 Banda Sea surface-layer divergence *Ocean Dynamics* **52** 2-10
[11] Siswanto and Suratno 2008 Seasonal pattern of wind induced upwelling over Java-Bali sea waters and surrounding area *International J. of Remote Sensing and Earth Science* **5** 46-56
[12] Kunarso, Hadi S, Ningsih N S and Baskoro M S 2011 Variabilitas suhu dan klorofil-a di daerah upwelling pada variasi kejadian ENSO dan IOD di perairan Selatan Jawa sampai Timor *Ilmu Kelautan* **16**(3) 171-180
[13] Wirasatriya A, Setiawan R Y and Subardjo P 2017 The Effect of ENSO on the Variability of Chlorophyll-a and Sea Surface Temperature in the Maluku Sea *IEEE Journal of Selected Topics in Applied Earth Observations and Remote Sensing* 1-6
[14] Madec G, Delecluse P, Imbard M and Levy C 1998 *OPA 8.1 Ocean General Circulation Reference Manual* (Paris: Institut Pierre Simon Laplace des sciences de l'Environnement Global)
[15] Emery W J and Thomson R E 2014 *Data analysis methods in physical oceanography* (Waltham: Elsevier)
[16] Sterl A and Hazeleger W 2003 Coupled variability and air-sea interaction in the South Atlantic Ocean *Clim. Dyn*. **21** 550-571
[17] Tranchant B, Reffray G, Greiner E, Nugroho D, Koch-Larrouy A and Gaspar P 2015 Evaluation of an operational ocean model configuration at 1/12^{o} spatial resolution for the Indonesian seas-part 1:Ocean physics *Geoscient Mod. Develop*. 8:6611-6668.
[18] Atmadipoera A S and Hasanah P 2017 Characteristics and Variability of Flores ITF and its coherence with the South Java coastal current. *J. Ilmu dan Teknologi Kelautan Tropis* **9**(2) 537-556
[19] Steinke S, Prange M, Feist C, Groeneveld J and Mohtadi M 2014 Upwelling variability off southern Indonesia over the past two millennia *Geophys. Res. Lett*. **41** 7684–7693
[20] Steward R H 2008 *Introduction to Physical Oceanography* (Texas: Department of Oceanography Texas A & M University)
[21] Utama F G, Atmadipoera A S, Purba M, Sudjono E H, Zuraida R 2017 Analysis of Upwelling event in Southern Makassar Strait *IOP Conference Series: Earth and Environmental Science* **54** 012085 doi: 10.1088/1755-1315/54/1/012085
[22] Rosdiana A, Prartono T, Atmadipoera A S and Zuraida R 2017 Nutrient and chlorophyll-a distribution in Makassar upwelling region: from MAJAFLOX Cruise 2015 *IOP Conference Series: Earth and Environmental Science* **54** 012087. doi: 10.1088/1755-1315/54/1/012087
[23] Horhoruw S M, Atmadipoera A S, Nanlohy P and Nurjaya I W 2017 Anomaly of surface circulation and Ekman transport in Banda Sea during normal and ENSO episode (2008-2011) *IOP Conference Series: Earth and Environmental Science* **54** 012087. doi: 10.1088/1755-1315/54/1/012041
[24] Australian Bureau of Meteorology (BOM) Southern Oscillation Index (SOI) 2018 http://poama.bom.gov.au/climate/enso/enlist/index.shtml
[25] Jacox M G, Hazen E L, Zaba K D, Rudnick D L, Edwards C A, Moore A M and Bograd S J 2016 Impacts of the 2015-2016 El Nino on the California Current System: Early assessment and comparison to past events *Geophys. Res. Lett* **43**(13) 7072–7080
[26] L'Heureux M L, Takahashi K, Watkins A B, Barnston A G, Becker E J, Di Liberto T E, Gamble F, Gottschalck J, Halpert M S, Huang B, Mosquera-Vasquez K and Wittenberg A T 2017 Observing and Predicting the 2015/16 El Nino *Bulletin of the American Meteorological Society (BAMS)* 1363-1382 doi: 10.1175/BAMS-D-16-0009.1
[27] Atmadipoera A S, Molcard R, Madec G, Wijffels S, Sprintall J, Koch-Larrouy A, Jaya I and Supangat A 2009 Characteristics nad variability of the Indonesian Throughflow water at the outflow straits *Dee Sea Research I* **56** 1942-1954